

## $^{35}\text{Cl}$ NQR and Raman spectroscopy study of 4, 4'-dichlorobiphenyl

This article has been downloaded from IOPscience. Please scroll down to see the full text article.

1996 J. Phys.: Condens. Matter 8 3909

(<http://iopscience.iop.org/0953-8984/8/21/016>)

View [the table of contents for this issue](#), or go to the [journal homepage](#) for more

Download details:

IP Address: 171.66.16.208

The article was downloaded on 13/05/2010 at 16:41

Please note that [terms and conditions apply](#).

## <sup>35</sup>Cl NQR and Raman spectroscopy study of 4,4'-dichlorobiphenyl

J Schneider†§, A Wolfenson†, A Brunetti†|| and L A de O Nunes‡

† FaMAF, Universidad Nacional de Córdoba, Medina Allende y Haya de la Torre, Ciudad Universitaria, 5000 Córdoba, Argentina

‡ Instituto de Física de São Carlos, Universidade de São Paulo, Av. Dr Carlos Botelho 1465, Caixa Postal 369, CEP13560-970, São Carlos, SP, Brazil

Received 11 December 1995

**Abstract.** Pulsed <sup>35</sup>Cl nuclear quadrupole resonance (NQR) and Raman spectroscopy studies were performed to get information about the structural and dynamic thermal behaviour of the 4,4' dichlorobiphenyl. NQR measurements of the line-shape and the spin–lattice relaxation time  $T_1$  were obtained in the temperature range 80 K–320 K. Raman spectra from powder samples were recorded for temperatures between 4.5 K and 300 K. Although the morphology of the 4,4' dichlorobiphenyl molecule is very close to the biphenyl one, there is no evidence of any structural instability, such as the incommensurate phase transitions in biphenyl. Up to the lowest temperatures scanned, the compound seems to remain in the same crystalline ordered phase reported by x-ray diffraction at room temperature. The  $T_1$  and Raman measurements suggest that there are no significant dynamical changes (for example, the softening of a mode) in the scanned temperature range. Some considerations are made on the size of the para-substituents of biphenyl, the crystal packing and the stability of the periodic phases.

### 1. Introduction

The mechanisms that rule the equilibrium conformation of the biphenyl (C<sub>6</sub>H<sub>5</sub>)<sub>2</sub> molecule have been studied for several decades [1, 2]. In the gas phase the molecule has a dihedral angle  $\varphi$  between the two benzene rings of 42° [2]. Nevertheless, in the solid phase, the molecule is strongly affected by the crystalline potential and assumes a planar configuration ( $\varphi = 0^\circ$ ) at room temperature. The most interesting aspect, from the solid state physics point of view, is the instability of this conformation as temperature is lowered. A phase transition sequence from the crystalline ordered phase to two incommensurate phases (IC) was observed at 40 K and at 17 K [3, 4]. The dihedral angle in the IC phases becomes spatially modulated along the crystallographic  $b$  axis direction. The IC transitions arise from the competition between intramolecular forces (*ortho* hydrogen steric repulsion and conjugation of  $\pi$  electrons) and intermolecular forces among neighbour molecules [3]. From the applied chemistry point of view, the study of chlorine substituents of biphenyl is a very interesting subject, because of the severe effects on the environment produced by these compounds. The biological activity of chlorinated biphenyls is directly related to the molecular conformation [5] (substitutions in *ortho* positions present lower bioactivity than in *para* positions) and the reorientational freedom of phenyl rings [6].

§ Holder of a fellowship from Concejo de Investigaciones Científicas y Tecnológicas (CONICET), Argentina.

|| Fellow of Concejo de Investigaciones Científicas y Tecnológicas (CONICET), Argentina.

In recent years, a chlorinated derivative of biphenyl showing an IC phase, 4,4'-dichlorobiphenylsulphone, was identified by  $^{35}\text{Cl}$  nuclear quadrupole resonance (NQR) [7, 8]. The nature of this incommensuration was explained assuming similar arguments as in the biphenyl case. Subsequent studies confirmed that the IC parameter is the dihedral angle [9, 10].

In order to analyse the effects of the biphenyl substitutions on the crystalline potential and, eventually, a periodicity loss of the crystalline phase, we have begun a study of the most simple chlorinated substituents by  $^{35}\text{Cl}$  NQR. In our first work [11], NQR and Raman measurements were performed in 4-chlorobiphenyl (CB) showing the existence of conformational disorder, associated with a spread in the dihedral angle values.

4,4' dichlorobiphenyl (DCB) is the simplest and most symmetric di-chlorine substituent of biphenyl. The x-ray diffraction data of DCB [12] report at room temperature a monoclinic structure  $P2_1/n$  with eight molecules in the unit cell. The aim of the present work was to verify whether this periodic crystalline phase becomes unstable at lower temperatures, taking into account the structural temperature behaviour of biphenyl and 4-chlorobiphenyl. The  $^{35}\text{Cl}$  NQR is a very suitable technique to detect periodicity loss or disorder degrees in solid phases, due to the sensitivity of the electric field gradient (EFG) to any structural change. The NQR spectra and the spin-lattice relaxation time  $T_1$  of DCB were measured as a function of the temperature from 80 K to room temperature. In addition, the Raman spectroscopy provides direct information about the molecular dynamics, especially on low-frequency processes. Raman spectra were recorded from 5 K to room temperature.

According to the experimental results, some considerations about the substitution effects on molecular conformation and crystal packing of chlorinated biphenyls are discussed.

## 2. Experimental details

The specimen of DCB was obtained from Riedel-de-Haën (purity: 99%). The powder sample was sealed in a glass cylinder of length 1 cm and diameter 0.8 cm. Measurements of NQR from  $^{35}\text{Cl}$  frequency and  $T_1$  as a function of temperature were performed between 80 K and room temperature. The home-made spectrometer based on the pulse method, has been described in [13]. NQR spectra were obtained from the fast Fourier transform (FFT) of the digitized echo after a  $90^\circ - \tau_E - 180^\circ$  pulse sequence with a  $90^\circ$  pulse length between 20  $\mu\text{s}$  and 25  $\mu\text{s}$ . The characteristic value of  $\tau_E$  was 200  $\mu\text{s}$ . Sampling frequencies of the nuclear signal between 200 kHz and 20 MHz were used. The measurements were performed using the transmitter maximum peak power of 150 W. Measurements of  $T_1$  were made on the echo by the standard pulse sequence ( $90^\circ - \tau - 90^\circ - \tau_E - 180^\circ$ ), with separation times  $\tau$  varying from 0.1 ms to 5  $T_1$ . Each  $T_1$  value determination was performed with a minimum of 30  $\tau$  values and a maximum of 50. The NQR spectrometer temperature control provides temperature stability better than 0.1 K during the whole experiment.

Raman measurements for powder CB samples were carried out by using the 488 nm line of an Ar-ion laser as an exciting source. A Spex double monochromator equipped with single-photon counting and a home-made data acquisition system was used for the detection of the scattered radiation. The temperature of the sample was controlled by a helium flux cryostat. The spectral resolution of the measurements was  $1 \text{ cm}^{-1}$ .

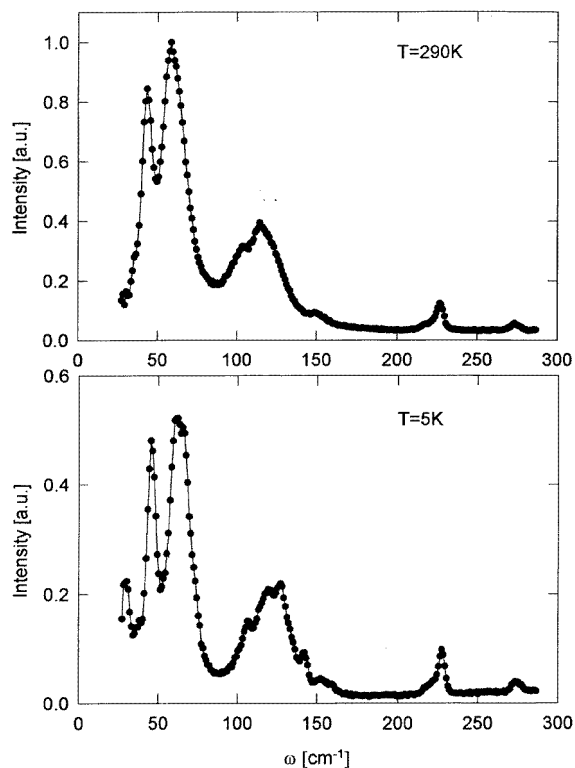


Figure 1. Low-frequency Raman spectra of a powder sample of DCB at 290 K and 5 K.

### 3. Experimental results

#### 3.1. Raman spectroscopy

Raman spectra of CB were recorded in the range  $30\text{ cm}^{-1}$ – $300\text{ cm}^{-1}$  from 4.8 K up to room temperature. Figure 1 shows two typical Raman spectra obtained at extreme scanned temperatures. A multiple-Lorentzian fit was performed on the measured spectra. The temperature dependence of the frequencies of the fitted Lorentzian is shown in figure 2. As can be seen, the temperature behaviour of the frequencies is linear in the whole temperature range. Least-squares fittings were performed on all the well resolved lines. The resulting parameters are summarized in table 1, indicating the fittings' temperature range. As can be seen in figures 1 and 2, there are no relevant dynamical changes in the whole temperature range.

#### 3.2. $^{35}\text{Cl}$ NQR spectrum

Figure 3(a) shows the observed NQR spectrum of DCB at 82 K. There are four NQR lines associated with the four chemically inequivalent chlorine sites. Each line was fitted with a Lorentzian function using the PeakFit software (Jandel Scientific). Figure 4 shows the temperature behaviour of the frequencies of the fitted Lorentzians. The NQR frequencies of the four lines decrease monotonically in the whole scanned temperature range. There is no evidence of any phase transition nor any other relevant dynamical change. This

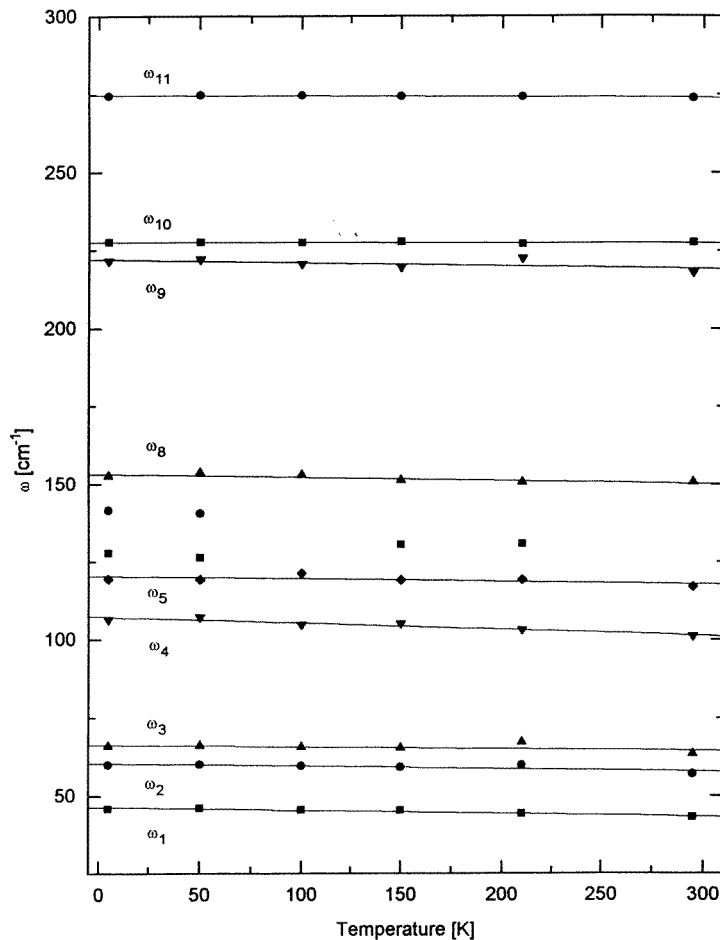


**Figure 2.** Temperature dependence of the frequencies of the resolved peaks of Raman spectra. Points: experimental data. Solid lines: linear fittings.

**Table 1.** Fittings of the thermal parameters of the more intense low-frequency Raman lines of DCB:  $\omega = \omega_0(1 - gT)$ . The numeration identifying the lines is according to figure 2.

Raman line	$\omega_0$ (cm <sup>-1</sup> )	$g \times 10^4$ (K <sup>-1</sup> )
$\omega_1$	$46.4 \pm 0.2$	$1.9 \pm 0.2$
$\omega_2$	$60.4 \pm 0.5$	$1.3 \pm 0.5$
$\omega_3$	$66.4 \pm 0.8$	$0.8 \pm 0.7$
$\omega_4$	$107.3 \pm 0.5$	$1.9 \pm 0.3$
$\omega_5$	$120.4 \pm 0.8$	$0.7 \pm 0.4$
$\omega_8$	$153.2 \pm 0.5$	$0.7 \pm 0.2$
$\omega_9$	$222 \pm 1$	$0.5 \pm 0.3$
$\omega_{11}$	$274.8 \pm 0.1$	$0.10 \pm 0.03$

indicates that the DCB remains in the whole temperature range in the crystalline ordered phase resolved by x-ray diffraction at room temperature [12]. The observed temperature

dependence of the NQR frequencies is typical for molecular solids in crystalline phases and can be reproduced by the Bayer–Kushida model of molecular torsional oscillations [14]. Following this model, the NQR frequency can be expressed as

$$\nu(T) = \nu_0 \left( 1 - \frac{3}{4} \hbar \sum_i \frac{1}{I_i \omega_i} \coth \left[ \frac{\hbar \omega_i}{2k_B T} \right] \right). \quad (1)$$

The summation index  $i$  ranges over all the oscillating modes involved in the effective EFG averaging [14]. The frequencies of the modes are  $\omega_i = \omega_{0i}(1 - g_i T)$ ,  $I_i$  are coefficients with units of moment of inertia and  $\nu_0$  is the limiting static value of the NQR frequency. The expression (1) was fitted to the experimental data, assuming only one dominant mode. A least-squares fit of the NQR data yields the parameters shown in table 2. The solid lines plotted in figure 4 represent these Bayer–Kushida fittings. The obtained values for parameter  $i$  are very close to the calculated moment of inertia of a rigid DCB molecule along an axis perpendicular to the Cl–Cl direction:  $I_x \approx 2840$  a.m.u.  $\text{\AA}^2$  and  $I_y \approx 2760$  a.m.u.  $\text{\AA}^2$ . This agreement suggests that the effective EFG dynamical averaging at Cl sites could be well explained assuming oscillations perpendicular to the symmetry axis of an almost rigid DCB molecule. The fitted values for the frequencies  $\omega_0$  agree with the broad structure in the Raman spectrum around  $120 \text{ cm}^{-1}$ , characterized by the main peaks  $\omega_4$  and  $\omega_5$ , with parameters  $\omega_{0-4} = 107.3 \text{ cm}^{-1}$  and  $\omega_{0-5} = 120.4 \text{ cm}^{-1}$ .

**Table 2.** Fitting parameters of the Bayer–Kushida expression (1) for the four NQR lines of DCB.

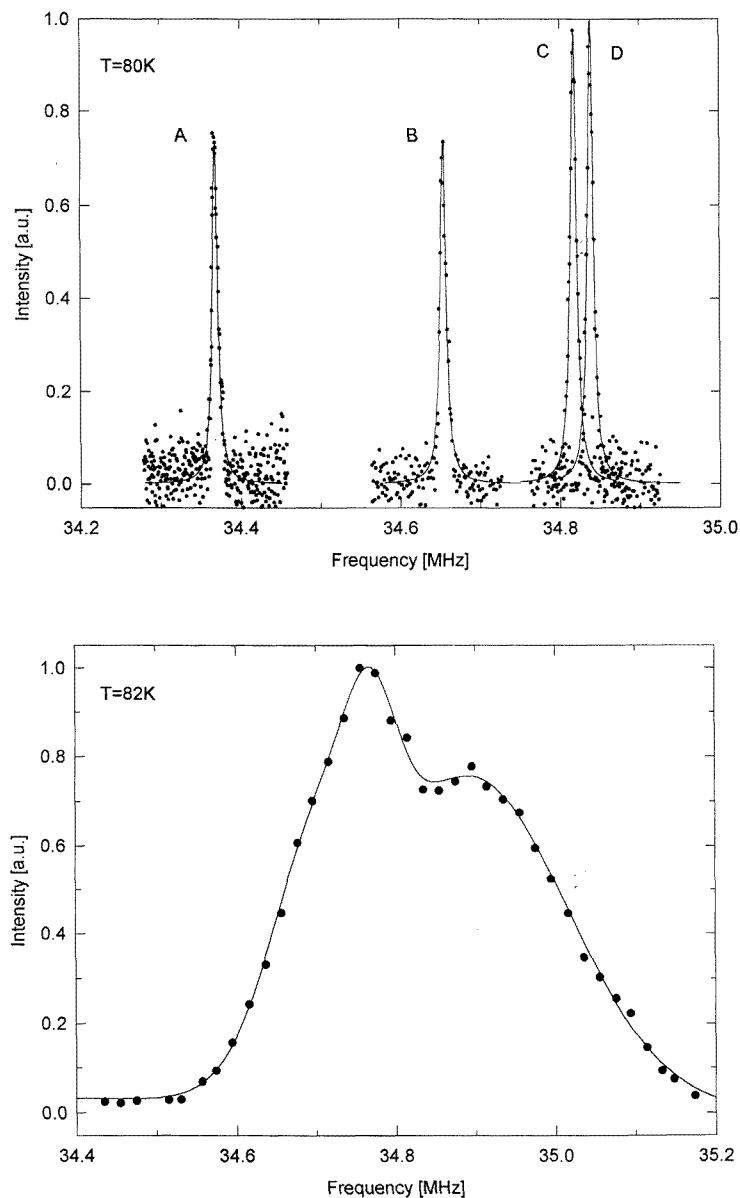
Line	$\omega^0$ ( $\text{cm}^{-1}$ )	$I$ (a.m.u. $\text{\AA}^2$ )	$\nu_0$ (MHz)	$g \times 10^4$ ( $\text{K}^{-1}$ )
A	120	2870	34.47	7
B	120	2600	34.77	7
C	110	2400	34.96	5.6
D	120	2400	34.97	5.9

Table 2 shows a similarity between the parameters of lines A–B and C–D. The values of dynamical parameters of the pair A–B are higher than those of the pair C–D. Furthermore, both ratios of area A:B and C:D are indistinguishable from unity in the whole temperature range, indicating the same number of chlorine sites contributing to lines A–B and C–D. These facts, and the determination by x-ray diffraction of two independent molecules in the unit cell [12], suggest a possible identification of the observed NQR lines. Each pair (AB and CD) could be associated with these two distinct molecules, and each line of the pair could be associated with the two chlorine atoms of the same molecule.

### 3.3. Spin–lattice relaxation time ( $T_1$ )

The spin–lattice relaxation time was measured saturating the frequencies corresponding to each peak of the spectrum. Figure 5 shows the temperature dependence of the measured  $T_1$  values. The order of magnitude of all  $T_1$  values (almost 1 second at liquid nitrogen temperatures) indicate that there are no low-frequency dynamical processes dominating the spin–lattice relaxation such as, for example, the softening of a mode. The log–log plots in figure 5 show a linear temperature dependence of  $T_1$  values in the whole temperature range. This kind of behaviour is associated with the molecular torsional oscillation mode [14]:

$$\frac{1}{T_1} = AT^\lambda \quad (2)$$



**Figure 3.** (a) The NQR spectrum of 4,4'-dichlorobiphenyl at 80 K obtained from the measured echoes saturating each line. Points: experimental data. Solid lines: fitted Lorentzian function. (b) The broad NQR spectrum of 4-chlorobiphenyl at 82 K obtained from recording the echo signal at different irradiation frequencies.

usual values of  $\lambda$  in ordered molecular crystals are slightly above two. The parameters resulting from the fittings are shown in table 3. All the exponents  $\lambda$  have standard values for molecular crystals. As can be seen from the values of  $\lambda$ , the dynamic of fluctuations is slightly different between the chlorine sites corresponding to lines A–C and B–D.

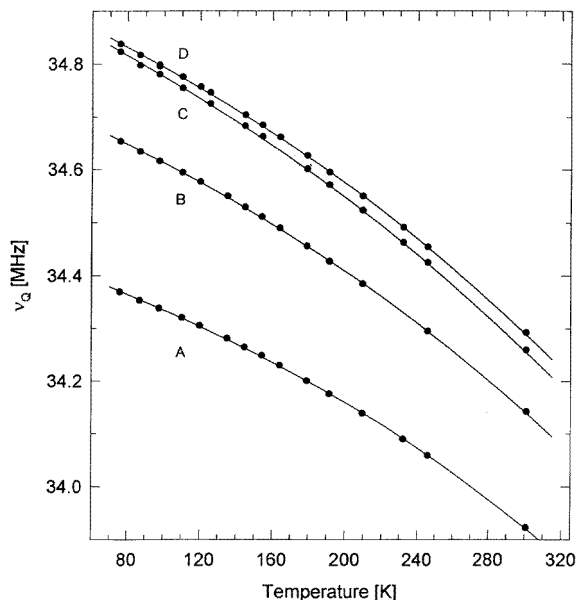


**Figure 4.** Temperature behaviour of the observed NQR frequencies of DCB. Points: experimental data. Solid lines: Bayer fittings.

**Table 3.** Fitting parameters of expression (2) for  $T_1$  values corresponding to lines A–D.

Line	$A \times 10^{-6}$ (mS K <sup>2</sup> )	$\lambda$
A	$40 \pm 10$	$2.5 \pm 0.1$
B	$6 \pm 2$	$2.2 \pm 0.1$
C	$45 \pm 5$	$2.54 \pm 0.02$
D	$9 \pm 1$	$2.22 \pm 0.03$

From these results, there is no evidence of phase transitions or activation of any dynamical process that enhances the spin–lattice relaxation in the scanned temperature range.

#### 4. Discussion

The NQR results show that the structure of solid DCB retains its periodicity in the temperature range 80 K–room temperature. This normal behaviour contrasts markedly with the observed one in several other compounds of the biphenyl family. As was mentioned in the introduction, the two closest members of the family, biphenyl and 4-chlorobiphenyl, show a loss of periodicity associated with a spread of dihedral angle values. The dihedral angle spatial distribution is incommensurate in biphenyl and random in 4-chlorobiphenyl. The disorder in 4-chlorobiphenyl is revealed by a broad NQR spectrum, due to the dispersion in the EFG values at the chlorine sites, as can be seen in figure 3(b). The periodicity loss in both compounds arises from the competition between inter and intramolecular interactions. Therefore, the behaviour observed in DCB suggests that para di-chlorine substitutions cause strong effects in the structural properties of the solid phase. The dihedral angle value of the DCB molecule is  $\varphi = 39.42^\circ$  in the solid phase [12], which is very close to the value of



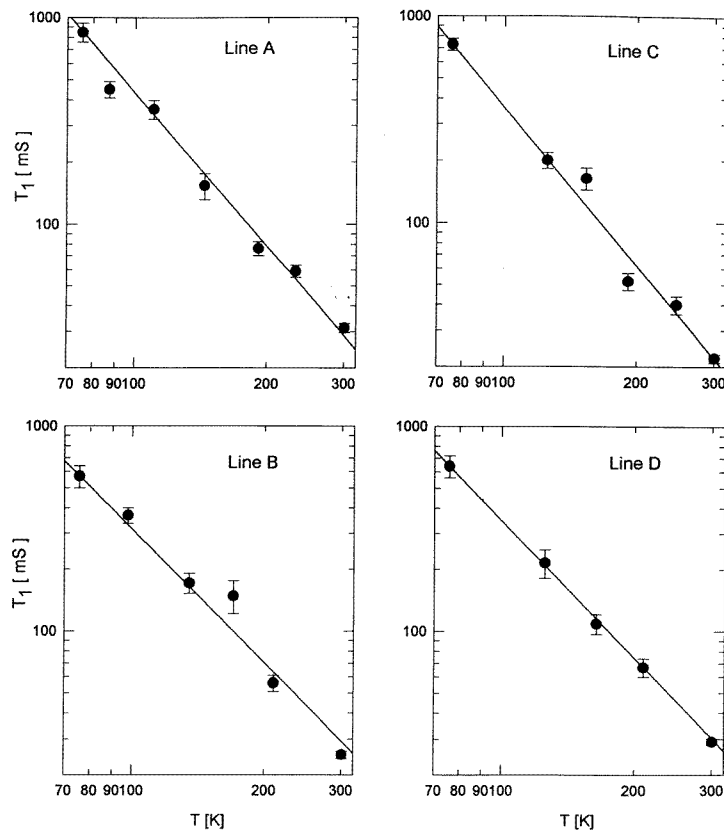


**Figure 5.** Temperature behaviour of the spin–lattice relaxation time of each NQR line of DCB. Points: experimental data. Solid lines: fitting of the torsional oscillation expression  $T_1 = AT^{-\lambda}$ .

$\varphi = 42^\circ$  observed in free biphenyl molecules. This similarity could be mainly originated by two different facts: a greater rigidity of the DCB molecule (a substitution effect of internal type) or a lower intermolecular interaction (a substitution effect on the crystalline packing).

**Table 4.** Crystallographic data of some biphenyl para di-substituents.

4,4' atoms	Space group	$V_c/Z$ ( $\text{\AA}^3$ )	$\varphi$ ( $^\circ$ )
H,H	$P2_1/a$	216.5	0
F,F	$P2_1/a$	227.2	0
Br,Br	$P2_1/n$	269.8	38.4
Cl,Cl	$P2_1/n$	260.9	39.42
CH <sub>3</sub> ,CH <sub>3</sub>	$P2_1/n$	268.3	36.4

In order to shed some light on the problem, a structure comparison among several para di-substituents was performed. Table 4 shows the space group, the  $\varphi$  value and the cell volume per molecule ( $V_c/Z$ ), a measure of the crystal packing efficiency. Following Pratt Brock *et al* [12], two well defined groups can be observed:

- (i) the compounds with space group  $P2_1/n$ , twisted molecular conformation ( $\varphi \cong 40^\circ$ )

and a  $V_c/Z$  value around  $270 \text{ \AA}^3$ ;

(ii) the compounds with space group  $P2_1/a$ , planar molecular conformation and a  $V_c/Z$  value around  $220 \text{ \AA}^3$ .

The compounds belonging to group I are characterized by an average volume of the substituent greater than those of group II. Due to the fact that in each of these groups there are substituents of different electronic nature (electron withdrawing and releasing), it is possible to conclude that the internal substitution effect is not dominant on the molecular conformation. Therefore, the size of the substituent atom or atomic group determines the crystal packing efficiency. Then, compounds with smaller atomic radius, like 4,4'-difluorobiphenyl and biphenyl, show a more compact structure. Simultaneously, this dense packing enables stronger intermolecular effects, which leads to planar or nearly planar molecular conformations.

A lack of periodicity of the crystalline phases of biphenyl derivatives included in group I could not be expected, due to less dense molecular packing leads to less intense neighbour interaction. These kinds of interaction play a decisive role in the generation of structural instabilities. On the other hand, crystalline phases of type II eventually may exhibit some loss of periodicity at certain temperatures.

It is interesting to consider the structural parameters of the para mono-substituent 4-bromobiphenyl (BB) in the context of the preceding discussion. The crystallographic data [15] show a  $Pn2_1$  space group with  $V_c/Z = 240 \text{ \AA}^3$  and two possible molecular configurations with  $\varphi = 20.4^\circ$  or  $\varphi = 17.8^\circ$ . These data are compatible with the information shown in table 4. BB seems to have an intermediate behaviour between group I and II determined by the mono-substitution character and the greater atomic radius of the bromine atom ( $1.12 \text{ \AA}$ ) with respect to the chlorine atom ( $0.97 \text{ \AA}$ ). It could be reasonable to expect for the CB a perturbed molecular conformation similar to the observed one in BB, due to the slightly lower atomic radius of the chlorine than the bromine atom.

**Table 5.** Cell parameters of some substituted biphenyls.

	Biphenyl	4,4'-DCBS	4,4'-DCBP
$a$ ( $\text{\AA}$ )	8.12	7.5	25.17
$b$ ( $\text{\AA}$ )	5.63	11.46	6.10
$c$ ( $\text{\AA}$ )	9.51	22.2	7.54
$V_c/Z$ ( $\text{\AA}^3$ )	216.5	306.4	289.4

Finally, it is possible to consider the behaviour of another type of substituted biphenyl, those sometimes called 'butterfly-like molecules': a central molecular group joining two phenyl rings. By means of  $^{35}\text{Cl}$  NQR measurements, some kind of instability of the crystalline ordered room-temperature phase was detected in 4,4' dichlorobiphenylsulphone [8] (DCBS) and in 4,4' dichlorobenzophenone [16] (DCBP), as temperature was lowered. The molecular conformation of these compounds is very different to those considered in table 4. The central molecular group determines a bending angle of  $104.6^\circ$  in DCBS [17] and  $121^\circ$  in DCBP [18] in the room-temperature crystalline phases. As was mentioned above, an IC phase transition occurs in DCBS from a crystalline ordered phase ( $I2/a$ , four molecules per cell), involving a modulation of the dihedral angle along the crystallographic  $b$  axis. In DCBP, the room-temperature crystalline structure ( $C2/c$ , four molecules per cell) becomes unstable at about 195 K. A first-order phase transition to a less symmetric conformational structure was observed [19]. Lowering the temperature below 180 K, another

first-order phase transition to a structure very close to the room-temperature phase was detected [19]. Although some authors proposed that this intermediate-temperature phase could be an incommensurate one [20], the structural changes affecting the dihedral angle of the molecules have not been clearly determined. Table 5 shows the cell parameters of biphenyl, DCBS and DCBP. DCBS and DCBP have  $V_c/Z$  values greater than those found in biphenyl or in the compounds of table 5. However, the length of each cell along the same direction of the molecular symmetry axis takes small values in the three cases: 5.63 Å in biphenyl, 7.5 Å in DCBS and 6.1 Å in DCBP. The shape of these molecules favours dense packing along the symmetry axis. The benzene rings of the molecules are closer along this direction, enhancing the intermolecular interactions and leading to the possibility that periodic phases become unstable as temperature is changed. The instability in DCBS and biphenyl (for temperatures lower than 21 K) is a collective process along the direction of maximum packing.

## 5. Conclusions

The NQR measurements show that 4,4' dichlorobiphenyl remains in its room-temperature crystalline ordered phase in the whole scanned temperature range. This behaviour is consistent with the assumption of weak intermolecular effects on the molecular conformation.

The chlorine substitution in 4,4' dichlorobiphenyl seems to affect mainly the crystal packing, by a volume type effect. A more compact crystal packing implies a stronger intermolecular interaction and, consequently, a more distorted molecular conformation in the solid state.

## Acknowledgments

The authors acknowledge financial support from the Concejo Nacional de Investigaciones Científicas y Técnicas (CONICET) and from the Concejo de Investigaciones de la Provincia de Córdoba (CONICOR), Argentina, Fundação de Amparo à Pesquisa do Estado de São Paulo (FAPESP), Brazil and Conselho Nacional de Desenvolvimento Científico e Tecnológico (CNPq), Brazil.

## References

- [1] Almenningen A and Bastiansen O 1958 *K. Nor. Vidensk. Selsk. Skr.* **4** 1
- [2] Hargreaves A and Rizvi S 1962 *Acta Crystallogr.* **15** 365
- [3] Heine V and Price S 1985 *J. Phys. C: Solid State Phys.* **18** 5259
- [4] Benkert C and Heine V 1987 *J. Phys. C: Solid State Phys.* **20** 3355
- [5] Holan G and Spurling T 1974 *Experientia* **30** 480
- [6] Tang T, Nowakowska M, Guillet J and Csizmadia I 1991 *J. Mol. Struct. (Theochem.)* **232** 133
- [7] Corberó J, Wolfenson A, Pusiol D and Brunetti A 1986 *Phys. Lett.* **114A** 105
- [8] Pusiol D, Wolfenson A and Brunetti A 1989 *Phys. Rev. B* **40** 2523
- [9] Kasano H, Koshiba T, Kasatani H and Terauchi H 1990 *J. Phys. Soc. Japan* **59** 408
- [10] Zúñiga F, Perez-Mato J and Breczewski T 1993 *Acta Crystallogr. B* **49** 1060
- [11] Schneider J, Wolfenson A, Schürer C, Brunetti A and Nunes L A O 1996 *Phys. Rev. B* **53** 9045
- [12] Pratt Brock C, Kuo M and Levy H 1978 *Acta Crystallogr. B* **34** 981
- [13] Pusiol D and Brunetti H 1984 *J. Phys. C: Solid State Phys.* **17** 4487
- [14] Chihara H and Nakamura N 1981 *Advances in Nuclear Quadrupole Resonance* vol IV, ed J A S Smith (London: Heiden) p 1
- [15] Pratt Brock C 1980 *Acta Crystallogr. B* **36** 968

- [16] Schneider J, Wolfenson A and Brunetti A 1992 *J. Phys.: Condens. Matter* **4** L571
- [17] Sime G and Abrahms C 1960 *Acta Crystallogr.* **13** 1
- [18] Granger M and Coillot M 1985 *Acta Crystallogr.* **41** 542
- [19] Peretti P and Ranson P 1979 *J. Raman Spectrosc.* **8** 209
- [20] Wolfenson A, Pusiol D and Brunetti A 1990 *Z. Naturf. a* **45** 334